# Research of the Dehydration Process of Amber-Containing Mining Mass

*Valerii KORNIIENKO[1)], Yevhenii MALANCHUK[2)], Vitalii ZAIETS[3)], Vasyl SEMENIUK[4)], Myroslava KUCHERUK[5)]*

[1)] Doctor of Engineering, Professor, Department of Mineral Deposits Development and Mining Engineering, National University of Water and Environmental Engineering, Soborna str, 11, Rivne, Ukraine; ORCID https://orcid.org/0000-0002-7921-2473
[2)] Doctor of Engineering, Professor, Department of Automation, Electrical Engineering and Computer-Integrated Technologies, National University of Water and Environmental Engineering, Soborna str, 11, Rivne, Ukraine; ORCID https://orcid.org/0000-0001-9352-4548
[3)] PhD, Associate Professor, Department of Mineral Deposits Development and Mining Engineering, National University of Water and Environmental Engineering, Soborna str, 11, Rivne, Ukraine; ORCID https://orcid.org/0000-0003-0659-7402; email:v.v.zayets@nuwm.edu.ua
[4)] Senior Lecturer, Department of Development of Deposits and Mining,National University of Water and Environmental Engineering, Soborna str, 11, Rivne, Ukraine; ORCID https://orcid.org/0000-0002-2348-3143
[5)] Senior Lecturer, Department of Development of Deposits and Mining,National University of Water and Environmental Engineering, Soborna str, 11, Rivne, Ukraine; ORCID https://orcid.org/0000-0002-0443-9139

http://doi.org/10.29227/IM-2023-01-01

Submission date: 02-02-2023 | Review date: 13-03-2023

## *Abstract*

*The article highlights the results of research into the process of dehydration of amber-containing mining mass using a vibroclassifier. Features of the technological scheme of amber extraction are described, as it relates to water supply points. The state of equilibrium of the liquid in the cell of the vibroclassifier under different conditions of sieve wettability was studied: a liquid that does not wet the sieve fibers; liquid that wets the fibers of the sieve; a thin film of liquid that wets the sieve fibers.*

*As a result of the research, it was established that in the case when the liquid does not wet the fibers of the sieve, the height of the layer of liquid that is maximally retained in the cell is at least 3 times greater than in the case of the liquid that wets the fibers of the sieve. The reliability of the obtained results is confirmed by the use of proven research methods and a relative error between calculated and experimental values at the level of 20%.*

**Keywords:** *amber, vibroclassifier, sieve cell, dehydration*

**Introduction**

The technology and equipment offered by us for the extraction of amber from the mining mass is carried out, to a large extent, to implement the requirements for increasing the extraction of amber due to the processing of off-balance reserves in man-made deposits and improving the ecological situation of the environment [1]. This technology of amber extraction has a number of advantages over the existing ones (hydraulic and well technologies), but for a full assessment of its economic efficiency, it is necessary to determine a number of influential factors that were considered in other works [2–5]. The paper [2] considered the technology of classification and calculation of the water-sludge scheme. With the use of computer modeling, a program for calculating the water-sludge operation scheme of the vibroclassifier was developed. It allows you to determine the indicators of the classification products under different modes of operation. According to this technology, the raw feed is mixed with water in a mixer and submitted for classification in a vibroclassifier of complex action, the discharge of which is sent to dewatering classification on a vibrating screen. The sands of the vibroclassifier and the over-sieve product of the vibroscreen are removed as waste. After screening, the sieved product is returned to the feeder of the vibroclassifier in the form of a circulating load.

Amber extraction technology has two main features. The first refers to the points of introduction of additional (fresh) water and the saving of total water consumption, and the second – to the volume of the circulating load.

The technological scheme uses two fresh water supply points.

First, in the mixer, where it is mixed with the mining mass, since it is not possible to introduce dry feed into the classifier.

Secondly, water is introduced directly into the bath of the classifier. At this point, the supply of fresh water is necessary, since it is the main factor that allows you to adjust the density of the pulp in the bath, the volume of the drain, the speed of the upward flow and the amount of circulating load.

The circulating load is the sublattice product of the dewatering screen. The magnitude of this load (further – circulation) can theoretically reach 100% of the power supply or more. However, in practice, it cannot be kept within high limits for two reasons: the first reason is that with high circulation, the density of the suspension in the classifier bath will decrease; the second – the volume of the downpour will increase and, accordingly, the speed of the upward flow. Due to this, larger fractions of the rock will be carried out in the drain and their number will increase. This is a negative factor – instead of removing the empty rock from the process, we organize its circulation in the scheme.

Note that the rational range of pulp density in the bath is 1400–1600 g/l. The calculation of technology parameters is performed for the upper limit of density, that is, for "hard" conditions, based on the need to reduce water consumption to ensure the amber extraction process.

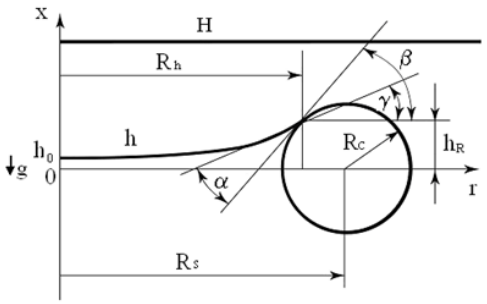


Fig. 1. Calculation diagram of the equilibrium of the liquid layer that does not wet the mesh fibers
Rys. 1. Schemat obliczeniowy równowagi warstwy cieczy, która nie zwilża włókien siatki

The study of the process of dehydration during the classification of the mining mass allows to evaluate the efficiency of the equipment in the extraction and processing of amber.

**Study of liquid equilibrium in vibroclassifier cell**

Various mineral processing technologies involve classification of the rock mass in the form of pulp and subsequent dehydration of the classification products on sieving surfaces in the form of nets. For this purpose, both stationary devices and a number of modifications of vibrating screens have been created and continue to be improved. At the same time, one of the most important engineering tasks is to increase the efficiency of classification and dewatering on sieving surfaces. The greatest difficulty is caused by the screening of the rock mass with a grain size in the range from 5.0 mm to 50 microns. This is due to the formation of a film of liquid in the cells of the sieve, which makes it difficult to screen the pulp, which significantly reduces the efficiency of the process. The practice of using various sieving surfaces during pulp classification indicates the need for intensive dynamic excitation of this surface.

Therefore, it is relevant to determine the dependence of the efficiency of dehydration in the classification of mining mass on the specified factors.

The study of the equilibrium of liquids with free surfaces has long attracted the attention of researchers and forms a separate section of hydromechanics, which considers the forms of equilibrium of liquid in capillaries, the forms of equilibrium of drops on surfaces, capillary surfaces without gravity, contact angles of the liquid with the walls of the container. Equilibrium changes in the capillary fluid are the subject of research by various authors. In it, mathematical models of equilibrium figures are built, and the stability of various changes is determined. In some fundamental works, a wide range of tasks related to weightlessness and the hydromechanics of a liquid rotating under weak gravity is considered. In the studies presented in this article, the problems related to the equilibrium of a liquid with known capillary properties are considered. These studies were conducted under the supervision of Doctor of Technical Engineering, Prof. V.P. Nadutiy (Institute of Geotechnical Mechanics named by N. Poljakov, Dnipro, Ukraine) jointly with scientists of the National University of Water and Environmental Engineering (Rivne, Ukraine) both in laboratories and in field conditions at facilities in the Rivne region (Ukraine). Without going into the nature of capillarity and using known provisions, we consider the equilibrium layers of liquid in a cell formed by a fiber that can be wetted or not wetted by a stationary liquid. The hydrostatics equation is the basis for the performance of the tasks on the equilibrium of immobile capillary liquids

$$dp/dx=\pm\rho g \tag{1}$$

where x is the coordinate, m;
ρ – liquid density, kg/m$^3$;
$g$ – acceleration of the free fall of the body, m/s$^2$;
$p$ – pressure, Pa.

Condition on the surface of phase separation

$$p_h - p_a = -\sigma\left[\frac{h''}{(1+(h')^2)^{3/2}} + \frac{h'}{r(1+(h')^2)^{1/2}}\right] \tag{2}$$

where r is the radius, m;
$p_a$ – atmospheric pressure, Pa;
$p_h$ – pressure on the free surface of the liquid, Pa;
σ – coefficient of surface tension, N/m;
h – the coordinate x surface points, m.

A liquid that does not wet the fibers of the sieve. In the case when the liquid does not wet the material from which the mesh is made (Fig. 1), after integrating equation (1) from the lower surface h to the upper surface H, which is also under atmospheric pressure, and taking into account the direction of the x axis and the acceleration of free fall g, the equation of statics of the liquid layer in the sieve cell has the form

$$\frac{h''}{(1+(h')^2)^{3/2}} + \frac{h'}{r(1+(h')^2)^{1/2}} + \frac{\rho g}{\sigma}(h-H) = 0 \tag{3}$$

where a dash and two dashes denote the first and second derivatives of r, respectively.

After transformations of expression (3), the equilibrium equation in the sieve cell is obtained

$$h = H - \frac{R_h\theta}{\kappa R_S J_1(\kappa)} J_0(\kappa n) \tag{4}$$

where $n=r/R_h$; $\bar{h}=h/R_S$; $\bar{H}=H/R_S$; - dimensionless quantities;
$R_c$ – radius of the mesh fiber, m;
$R_h$ – the radius of the circle along which the liquid contacts the surface of the fiber, m;
$R_S$ – the sum of the radii of the mesh fiber and the cell opening, m;
$h_0$ – height of the surface at the point n = 0, m;
$h_R$ – height of the surface at the point n = 1, m;

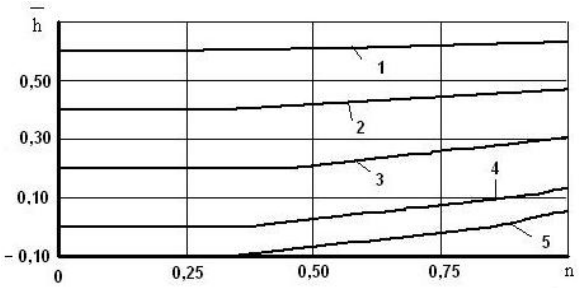


Fig. 2. Curves characterizing the shape of the lower free boundary of the liquid layers, which does not wet the mesh fibers: 1 – H=0.042 m; 2 – H=0.138 m; 3 – H=0.243 m; 4 – H=0.348 m; 5 – H=0.391 m

Rys. 2. Krzywe charakteryzujące kształt dolnej swobodnej granicy warstw cieczy, która nie zwilża włókien siatki: 1 – H=0.042 m; 2 – H=0.138 m; 3 – H=0.243 m; 4 – H=0.348 m; 5 – H=0.391 m

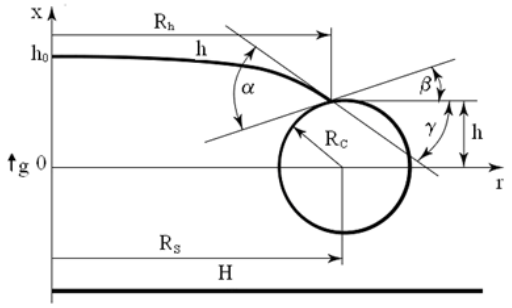


Fig. 3. Calculation diagram of the equilibrium of the liquid layer that wets the fiber in the grid cell

Rys. 3. Schemat obliczeniowy równowagi warstwy cieczy zwilżającej włókno w komórce siatki

θ=tgγ (γ is the angle between the liquid tangent to the surface at the point of engagement and the straight line parallel to the abscissa axis);

$J_0$– Bessel function of the first kind of zero order;

$\kappa=Bo^{1/2}$, $Bo=\rho g R h^2/\sigma$ – Bond number;

α – wetting angle;

β – the angle between the tangent to the fiber surface at the point of liquid engagement and the abscissa axis,

γ=β-α.

To determine the numerical values, it is necessary to set hR, then calculate $R_h$, tgβ and θ, after which H is determined. By performing such calculations, you can make sure that for some values $h_R^* \le h_R \le 1$ H≤0. Such a solution cannot exist physically, solutions of this problem begin at H≥1. If 0<H<1, we will get a problem about a drop "sitting" on a sieve cell. It requires a slightly different mathematical formulation and falls out of the class of tasks under consideration. Thus, the analytical approach determines what situations may arise during the numerical solution of this problem. In fig. 2. the results of the calculations are given in the form of curves characterizing the shape of the lower free boundary. Calculations were made for the following conditions: $R_C=50\cdot10^{-6}$ m, $R_S=75\cdot10^{-6}$ m, tgα=1, σ=0.072 N/m. The curves given in the figure correspond to different values of the height of the liquid layer H above the cell.

From fig. 2, it follows that with a decrease in $h_0$, the liquid layer retained by the grid cell increases, or more precisely, with an increase in the liquid layer above the cell, the liquid sinks deeper into the center of the cell, which is quite natural, but this becomes a limit at larger positive values of θ. With a further decrease in $h_0$, the solution ceases to exist, which means the loss of the static equilibrium state.

A liquid that wets the sieve fibers. For the liquid that wets the mesh fibers, the calculation scheme for determining the equilibrium of the layer has a slightly different form (Fig. 3). For ease of solution, the x-axis is pointing up, but in the same direction as g (the figure is upside down).

Integrating expression (1) within the appropriate limits, the following equation is obtained in a dimensionless form

$$\frac{h''}{\left[1+\left(h'/R_h/R_S\right)^2\right]^{3/2}}+\frac{h'}{n\left[1+\left(h'/R_h/R_S\right)^2\right]^{1/2}}+Bo(h+H)=0 \quad (5)$$

It differs from the equation of the already considered case only by a plus sign before the value H (for physically correct solutions, H must be greater than zero). Using an analytical solution that will look like this

$$h=-H-\frac{R_h\theta}{\kappa R_S J_1(\kappa)}J_0(\kappa n) \quad (6)$$

determine the values of $h_R$ at which the solution of the problem exists. For this case, solutions exist for tgα<θ<0.

In fig. 4 shows the curves of the lower limit of the liquid characterizing the equilibrium of the layers. The given curves correspond to different values of the height of the liquid layer above cell H. The calculations were performed for the same values of $R_C$, $R_S$, and α as in the previous case. From fig. 4, it follows that with a decrease in $h_0$, the height of the H layer increases, or more precisely, with an increase in the liquid layer, the lower limit lowers, however, there is also a limitation due to the fact that the liquid reaches the radius $R_S$.

Curve 3 in fig. 4 approaches this limiting value. A circle of radius $R_S$ separates liquids that are in equilibrium in neighboring cells. Upon contact, the equilibrium structure is disturbed and a film is formed that connects the cells of the sieve. This is a condition for the loss of stability of the structure un-

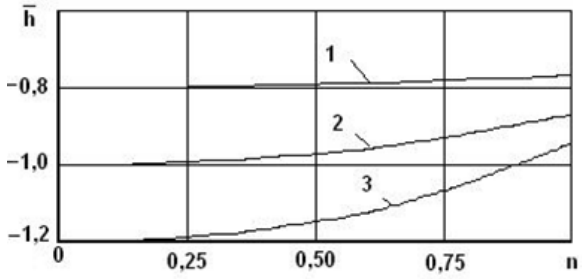


Fig. 4. Curves characterizing the shape of the lower free boundary of the liquid layers that wets the sieve fibers
1 – H = 0.031 m, 2 – H = 0.077 m, 3 – H = 0.109 m

Rys. 4. Krzywe charakteryzujące kształt dolnej swobodnej granicy warstw cieczy zwilżającej włókna sita
1 – H = 0.031 m, 2 – H = 0.077 m, 3 – H = 0.109 m

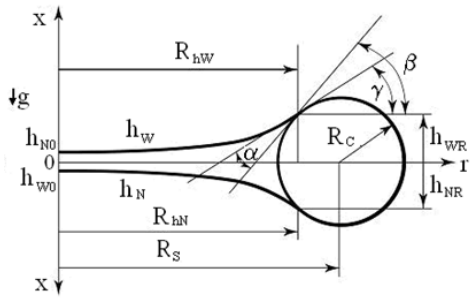


Fig. 5. Calculation diagram of the equilibrium in the cell of a thin film of liquid that wets the sieve fibers

Rys. 5. Schemat obliczeniowy równowagi w komórce cienkiej warstwy cieczy zwilżającej włókna sita

der consideration: the task undergoes qualitative changes in its formulation. Another case is possible when the value of H<1 is the presence of a thin film covering the cell.

A thin film of liquid that wets the fibers of the sieve. In fig. 5 schematically shows the specified case, which may be of practical interest, and fits into the formulated class of tasks. For ease of resolution, the x-axis in the upper and lower parts of the figure are directed in different directions (the lower part is viewed upside down). When integrating equation (1) over x, the equilibrium equation for the upper and lower surfaces is obtained in a dimensionless form

$$\frac{h''_W}{\left[1+\left(h'_W R_{hW}/R_S\right)^2\right]^{3/2}}+\frac{h'_W}{n\left[1+\left(h'_W R_{hW}/R_S\right)^2\right]^{1/2}}-Bo_W(h_W+H_W)=0 \quad (7)$$

$$\frac{h''_N}{\left[1+\left(h'_N R_{hN}/R_S\right)^2\right]^{3/2}}+\frac{h'_N}{n\left[1+\left(h'_N R_{hN}/R_S\right)^2\right]^{1/2}}+Bo_N(h_N-H_N)=0 \quad (8)$$

where the index W refers to the upper surface, and N – to the lower and $H_W=H_N=H=(p_a-p_0)/(\rho g R_S)$
$p_0$ – pressure at point x = 0, Pa.

When $B_o=0$, equations (7) and (8) become the same. This suggests that in weightlessness the boundaries of the surfaces are symmetrical. Discarding the quadratic terms in the denominators, the solution, using Bessel functions, will be written as

$$h_W=-H+\frac{R_{hW}\theta_W}{\kappa_W R_S J'_1(\kappa_W)}J'_0(\kappa_W n),\quad h_N=H-\frac{R_{hN}\theta_N}{\kappa_N R_S J_1(\kappa_N)}J_0(\kappa_N n) \quad (9)$$

Excluding H from these equations and assuming n=1, the relationship between the points of engagement of the lower and upper boundaries of the liquid with the fiber is obtained

$$h_{WR}+h_{NR}=\frac{R_{hW}\theta_W}{\kappa_W R_S J'_1(\kappa_W)}J'_0(\kappa_W)-\frac{R_{hN}\theta_N}{\kappa_N R_S J_1(\kappa_N)}J_0(\kappa_N) \quad (10)$$

In this equation, it is necessary to set the value of $h_{NR}$, then to calculate $h_{WR}$ by selection, and to calculate the shape of the upper and lower boundaries of the film according to equations (9). After calculating the Bond number for the parameters of interest, it was determined that its maximum value is $B_o=0.000766$ at $R_h=R_S$. In this regard, the lower and upper boundaries of the film are similar in shape. Calculations show that the values of the corresponding points of the calculated lower and upper surfaces differ from each other in the third order. In fig. 6 shows the curves of the surfaces of films with different volumes. It is calculated using analytical solutions (9), according to the following formula:

$$\begin{aligned}V_P=\pi\Big\{&(h_{RW}+h_{RN})(R_C^2+R_S^2)-R_C R_S^2\left[\arcsin\left(\frac{h_{RW}}{R_S}\right)+\arcsin\left(\frac{h_{NW}}{R_S}\right)\right]-\\&-R_C R_S\left[h_{RW}\left(1-\frac{h_{RW}^2}{R_S^2}\right)^{1/2}+h_{RN}\left(1-\frac{h_{RN}^2}{R_S^2}\right)^{1/2}\right]-\frac{1}{3}(h_{RW}^3+h_{RN}^3)\Big\}+\\&+2\pi\left\{R_{hW}^3\frac{\theta_W}{\kappa_W^2}\left[1-\frac{\kappa_W J'_0(\kappa_W)}{2J'_1(\kappa_W)}\right]-R_{hN}^3\frac{\theta_N}{\kappa_N^2}\left[1-\frac{\kappa_N J_0(\kappa_N)}{2J_1(\kappa_N)}\right]\right\}\end{aligned} \quad (11)$$

In fig. 6 shows the curves corresponding to some values of the volume of the liquid in the sieve cell.

Analyzing the data shown in fig. 6, it can be concluded that thinner films are characterized by concave surfaces (curves 1, 2). Surface 3 is almost straight, and curve 4 is convex, which characterizes the shape of the upper surfaces of liquid films.

**Conclusion**

As a result of the research, the equilibrium conditions of the liquid in the sieve cell of the vibroclassifier for fine-grained classification and dehydration were determined depen-

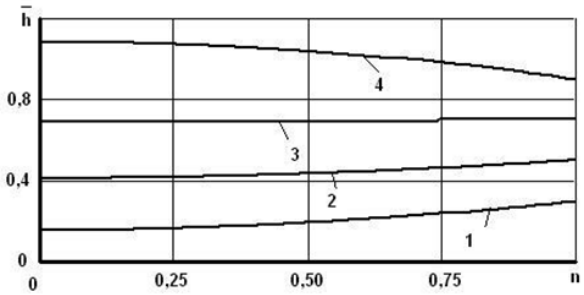


Fig. 6. Curves characterizing the shape of the upper surfaces of the films of the liquid that wets the mesh fibers: 1 – V=0.458·10$^{-10}$m$^3$; 2 – V=0.103·10-9m$^3$; 3 – V=0.193·10$^{-9}$m$^3$; 4 – V=0.407·10$^{-9}$m$^3$

Rys. 6. Krzywe charakteryzujące kształt górnych powierzchni warstw cieczy zwilżającej włókna siatki: 1 – V=0.458·10$^{-10}$m$^3$; 2 – V=0.103·10-9m$^3$; 3 – V=0.193·10$^{-9}$m$^3$; 4 – V=0.407·10$^{-9}$m$^3$

ding on the wetting conditions and the height of the liquid layer: in the case when the liquid does not wet the fibers of the sieve, the height of the liquid layer that is maximally retained in the cell is not less than 3 times the height of the layer held by the liquid wetting the sieve fibers.

The reliability and validity of scientific results are confirmed by the use of proven research methods, satisfactory convergence of calculated and experimental values with a relative error not exceeding 20%.

**Literatura – References**


1. Belichenko, O., & Ladzhun, J. (2016). Complex gemological research of new types of treated amber. Visnyk of Taras Shevchenko National University of Kyiv. Geology, 4(75), 30-34.https://doi.org/10.17721/1728-2713.75.04
2. Natkaniec-Nowak, L., Dumańska-Słowik, M., Naglik, B., Melnychuk, V., Krynickaya, M. B., Smoliński, W., & Ładoń, K. (2017). Depositional environment of Paleogen amber-bearing quartz-glauconite sands from Zdolbuniv (Rivne region, NW Ukraine): mineralogical and petrological evidences. Gospodarka Surowcami Mineralnymi, 33(4), 45-62.https://doi.org/10.1515/gospo-2017-0041
3. Alekseev, V.I. (2013). The beetles Baltic amber: The checklist of described species and preliminary analysis of biodiversity. Zoology and Ecology, 23(1), 5-12.https://doi.org/10.1080/21658005.2013.769717
4. Zakharenko, A.M., & Golokhvast, K.S. Using confocal laser scanning microscopy to study fossil inclusion in Baltic amber, a new approach. Key Engineering Materials, (806), 192-196. https://doi.org/10.4028/www.scientific.net/KEM.806.192
5. Zabyelina, Y., & Kalczynski, N. (2020). Shadowy deals with "sunny stone": Organized crime, informal mining, and the illicit trade of amber in Ukraine. Illegal Mining, 241-272.https://doi.org/10.1007/978-3-030-46327-4_9
6. Łazowski, L. (2007). The comments regarding usage and conservation of the amber resources. Przeglad Geologiczny, 55(8), 670-672.
7. Yakymchuk, N.A., Levashov, S.P., & Korchagin, I.N. (2019). New evidence of amber endogenous genesis. 18th International Conference on Geoinformatics – Theoretical and Applied Aspects.https://doi.org/10.3997/2214-4609.201902017
8. Krek, A., Ulyanova, M., & Koschavets, S. (2018). Influence of land-based Kaliningrad amber mining on coastal zone. Marine Pollution Bulletin, (131), 1-9.https://doi.org/10.1016/j.marpolbul.2018.03.042
9. Poulin, J., & Helwig, K. (2016). The characterization of amber from deposit sites in western and northern Canada. Journal of Archaeological Science: Reports, (7), 155-168.https://doi.org/10.1016/j.jasrep.2016.03.037
10. Xing, Q.Y., Yang, M., Yang, H.X., & Zu, E.D. (2013). Study on the gemological characteristics of amber from Myanmar and Chinese Fushun. Key Engineering Materials, (544), 172-177.https://doi.org/10.4028/www.scientific.net/KEM.544.172
11. Zhu, W.C., & Wei, C.H. (2010). Numerical simulation on mining-induced water inrushes related to geologic structures using a damage-based hydromechanical model. Environmental Earth Sciences, 62(1), 43-54.https://doi.org/10.1007/s12665-010-0494-6
12. Lemos, J.V., & Lorig, L.J. (2020). Hydromechanical modelling of jointed rock masses using the Distinct Element Method. Mechanics of Jointed and Faulted Rock, 605-612.https://doi.org/10.1201/9781003078975-85
13. Cappa, F., Guglielmi, Y., Fénart, P., Merrien-Soukatchoff, V., & Thoraval, A. (2005). Hydromechanical interactions in a fractured carbonate reservoir inferred from hydraulic and mechanical measurements. International Journal of Rock Mechanics and Mining Sciences, 42(2), 287-306.https://doi.org/10.1016/j.ijrmms.2004.11.006
14. Moshynsky, V. (2001). Modern water conditions in the northwest part of Ukraine: An analysis. Water Engineering and Management, 148(4), 22-26.
15. Burnashov, E., Chubarenko, B., & Stont, Z. (2010). Natural evolution of western shore of the sambian peninsula on completion of dumping from an amber mining plant. Archives of Hydroengineering and Environmental Mechanics, 57(2), 105-117.
16. Mikhlin, Y.V., & Zhupiev, A.L. (1997). An application of the ince algebraization to the stability of non-linear normal vibration modes. International Journal of Non-Linear Mechanics, 32(2), 393-409.https://doi.org/10.1016/s0020-7462(96)00047-9
17. Sorin, C. (2013). Research studyes on mining activity impact on the area focsanei scurtesti, case study vadu pasii, buzau county. SGEM Geoconference on Ecology, Economics, Education and Legislation.https://doi.org/10.5593/sgem2013/be5.v1/s20.112
18. Stupnik, M., Kolosov, V., Kalinichenko, V., & Pismennyi, S. (2014). Physical modeling of waste inclusions stability during mining of complex structured deposits. Progressive Technologies of Coal, Coalbed Methane, and Ores Mining, 25-30.https://doi.org/10.1201/b17547
19. Van der Werf, I.D., Fico, D., De Benedetto, G.E., Sabbatini, L. (2016). The molecular composition of Sicilian amber. Microchemical Journal, (125), 85-96.http://doi.org/10.1016/j.microc.2015.11.012
20. Korniyenko V.Ya., Vasylchuk O.Yu., Zaiets V.V., Semeniuk V.V., Khrystyuk A.O., Malanchuk Ye.Z. (2022). Research of amber extraction technology by vibroclassifier. IOP Conf. Ser.: Earth Environ. Sci. 1049 012027. https://doi.org/10.1088/1755-1315/1049/1/012027

21. Korniyenko V., Nadutyi V., Malanchuk Y., Yeluzakh M. (2020) Substantiating velocity of amber buoying to the surface of sludge-like rock mass. Mining of Mineral Deposits, 14(4), 90-96. DOI:https://doi.org/10.33271/mining14.04.090

22. Malanchuk Z., Korniyenko V., Malanchuk Ye., Khrystyuk A., Kozyar M. Identification of the process of hydromechanical extraction of amber. E3S Web of Conferences. Volume 166 (2020) 02008 DOI: https://doi.org/10.1051/e3sconf/202016602008

23. Malanchuk, Z., Korniienko, V., Malanchuk, Y., Moshynskyi, V. Analyzing vibration effect on amber buoying up velocity.E3S Web of Conferences 123, 01018 (2019). Ukrainian School of Mining Engineering - 2019. DOI: 10.1051/e3sconf/201912301018

24. Malanchuk, Y., Korniienko, V., Moshynskyi, V., Soroka V., Khrystyuk, A., Malanchuk, Z. Regularities of hydromechanical amber extraction from sandy deposits. Mining of mineral deposits. - 2019. DOI: 10.33271/mining13.01.049

25. Low-grawity Fluid Mechanics. Mathematical Theory of Capillary Phe-nomena / A.D. Myshkis, V.G. Babskii, N.D. Kopachevskii, L.A. Slobozhanin, A.D. Tyuptsov - Springer-Verlag Berlin, Heidelberg, New York, London, Paris, Tokyo, 1986. 602 pp.

26. Nadutyi, V., Korniyenko, V., Malanchuk, Z., Cholyshkina, O. Analytical presentation of the separation of dense suspensions for the extraction of amber. E3S Web of Conferences 109, 00059 (2019). Essays of Mining Science and Practice. DOI: 10.1051/e3sconf/20191090005

27. Malanchuk Z., Moshynskyi V., Martyniuk P., Stets S., Galiyev D. (2020) Modelling hydraulic mixture movement along the extraction chamber bottom in case of hydraulic washout of the tuff-stone. E3S Web of Conferences. Volume 211 (2020) 01011 DOI:https://doi.org/10.1051/e3sconf/202020101011

28. Sai, K., Malanchuk, Z., Petlovanyi, M., Saik, P., Lozynskyi, V. Research of thermodynamic conditions for gas hydrates formation from methane in the coal mines. Solid State Phenomena (2019). DOI: 10.4028/www.scientific.net/SSP.291.155.

## *Badanie procesu odwadniania mas wydobywczych zawierających bursztyn*

*W artykule przedstawiono wyniki badań procesu odwadniania masy wydobywczej zawierającej bursztyn, za pomocą wibroklasyfikatora. Opisano cechy schematu technologicznego wydobywania bursztynu w odniesieniu do punktów zaopatrzenia w wodę. Badano stan równowagi cieczy w komorze wibroklasyfikatora w różnych warunkach zwilżalności sita: ciecz niezwilżająca włókien sita; płyn zwilżający włókna sita; cienka warstwa cieczy zwilżającej włókna sita.*

*W wyniku przeprowadzonych badań ustalono, że w przypadku gdy ciecz nie zwilża włókien sita, wysokość maksymalnie zatrzymanej w komórce warstwy cieczy jest co najmniej 3 razy większa niż w przypadku cieczy zwilżającej włókna sita. Wiarygodność uzyskanych wyników potwierdza zastosowanie sprawdzonych metod badawczych oraz względny błąd pomiędzy wartościami obliczonymi a doświadczalnymi na poziomie 20%.*

**Słowa kluczowe:** *bursztyn, wibroklasyfikator, komora sitowa, odwadnianie*